

# Single Crystal Growth and Magnetic Properties of Mn-doped Bi<sub>2</sub>Se<sub>3</sub> and Sb<sub>2</sub>Se<sub>3</sub>

Jeongyong Choi<sup>1</sup>, Hee-Woong Lee<sup>2</sup>, Bong-Seo Kim<sup>2</sup>, Sungyool Choi<sup>1</sup>,  
Jiyoun Choi<sup>1</sup> and Sunglae Cho<sup>1\*</sup>

<sup>1</sup>Department of Physics, University of Ulsan, 680-749, Korea

<sup>2</sup>Advanced Electrical Materials Group, Korea Electrotechnology Research Institute, Korea

(Received 10 December 2004)

We have grown Mn-doped Bi<sub>2</sub>Se<sub>3</sub> and Sb<sub>2</sub>Se<sub>3</sub> single crystals using the temperature gradient solidification method. We report on the structural and magnetic properties of Mn-doped Bi<sub>2</sub>Se<sub>3</sub> and Sb<sub>2</sub>Se<sub>3</sub> compound semiconductors. The lattice constants of several percent Mn-doped Bi<sub>2</sub>Se<sub>3</sub> and Sb<sub>2</sub>Se<sub>3</sub> were slightly smaller than those of the un-doped samples due to the smaller Mn atomic radius (1.40 Å) than those of Bi (1.60 Å) and Sb (1.45 Å). Mn-doped Bi<sub>2</sub>Se<sub>3</sub> and Sb<sub>2</sub>Se<sub>3</sub> showed spin glass and paramagnetic properties, respectively.

**Key words :** magnetic semiconductor, thermoelectric, Bi<sub>2</sub>Se<sub>3</sub>, Sb<sub>2</sub>Se<sub>3</sub>

## 1. Introduction

Group V<sub>2</sub>-VI<sub>3</sub> compounds are known as good materials for room-temperature thermoelectric and thermomagnetic refrigeration and power generation. Bi<sub>2</sub>Se<sub>3</sub> are narrow-bandgap semiconductors with rhombohedral layered crystal structure; three Se-Bi-Se-Bi-Se sequences combine to make a unit cell [1]. They can be cleaved easily along planes perpendicular to the trigonal axis (i.e., along the basal planes) due to a weak van der Waals bonding between Se atoms over a strong covalent bonding between Bi and Se layers. On the other hand, Sb<sub>2</sub>Se<sub>3</sub> is a relatively wide-bandgap semiconductor (E<sub>g</sub> = 1.3 eV) with orthorhombic crystal structure [2].

Currently diluted ferromagnetic semiconductors (DFS), which are prepared by substituting transition metals into nonmagnetic semiconductors, have attracted the worldwide scientific interests for the possible spintronic devices. Ferromagnetism was observed in various systems such as group II-VI [3-5], III-V [6-8], and IV [9, 10], II-IV-V<sub>2</sub> [11], etc. It was also reported that Fe-doped Bi<sub>2</sub>Te<sub>3</sub> and V-doped Sb<sub>2</sub>Te<sub>3</sub> had ferromagnetic (FM) ordering at 12 and 22 K, respectively [12, 13]. Also, we observed that Mn-doped Bi<sub>2</sub>Te<sub>3</sub> and Sb<sub>2</sub>Te<sub>3</sub> had ferromagnetic ordering at T<sub>C</sub> = 10 and 17 K, respectively [14].

Here we report on the single crystal growth and

magnetic properties of Mn-doped group Bi<sub>2</sub>Se<sub>3</sub> and Sb<sub>2</sub>Se<sub>3</sub> compound semiconductors.

## 2. Experiment

Single crystalline Mn-doped Bi<sub>2</sub>Se<sub>3</sub> and Sb<sub>2</sub>Se<sub>3</sub> were prepared from high-purity (99.999%) manganese (Mn), bismuth (Bi), antimony (Sb) and selenium (Se) powders with particle sizes < -200 meshes to maximize the surface area and thereby enhance the reaction kinetics. First, the powders were weighed and loaded into thick walled quartz ampoules. The ampoules were then evacuated (< 10<sup>-6</sup> Torr) and sealed. After encapsulation, the sealed ampoules were mixed, loaded into a vertical furnace and heated slowly to form single phase. For single crystal growth, Bi<sub>2-x</sub>Mn<sub>x</sub>Se<sub>3</sub> and Sb<sub>2-x</sub>Mn<sub>x</sub>Se<sub>3</sub> were cooled from 800 °C to 600 °C at 1 °C/h and thereafter at 100 °C/h. This procedure resulted in single crystals approximately 8 mm in size. The compositions of Mn were determined using EPMA (Electron Probe Micro-Analyzer).

## 3. Results and Discussion

We have prepared Bi<sub>1.97</sub>Mn<sub>0.03</sub>Se<sub>3</sub> and Sb<sub>1.96</sub>Mn<sub>0.04</sub>Se<sub>3</sub> single crystals. In order to confirm the crystal structures of Bi<sub>1.97</sub>Mn<sub>0.03</sub>Se<sub>3</sub> and Sb<sub>1.96</sub>Mn<sub>0.04</sub>Se<sub>3</sub>, we performed  $\theta$ -2 $\theta$  powder X-ray diffraction (XRD) studies as shown in Fig. 1. We have carefully searched for intermetallic secondary

\*Corresponding author: Tel: +82-52-259-2322;

e-mail: slcho@mail.ulsan.ac.kr

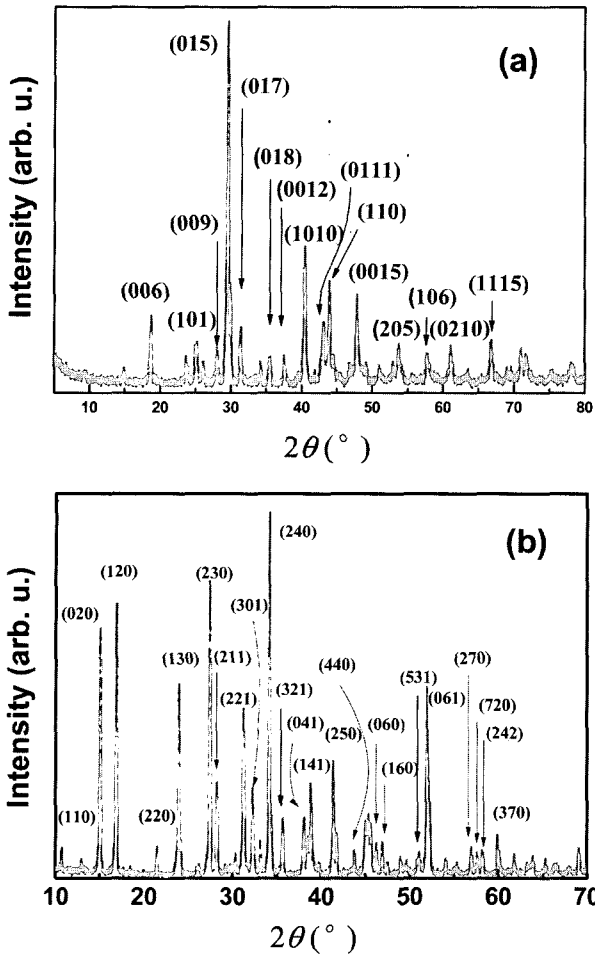


Fig. 1. Powder XRD patterns of (a)  $\text{Bi}_{1.97}\text{Mn}_{0.03}\text{Se}_3$  and (b)  $\text{Sb}_{1.96}\text{Mn}_{0.04}\text{Se}_3$  single crystals.

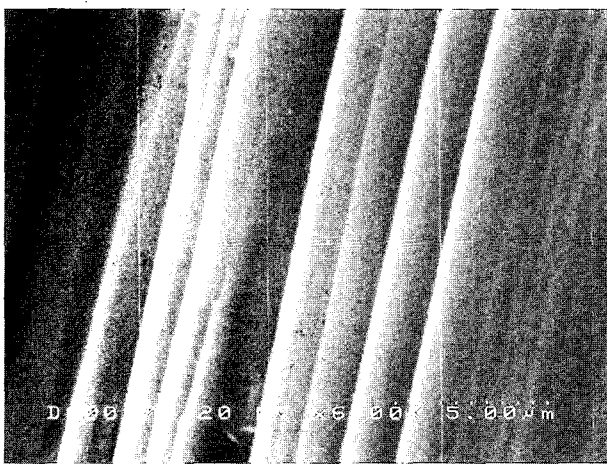


Fig. 2. The scanning electron microscopy (SEM) image of  $\text{Sb}_{1.96}\text{Mn}_{0.04}\text{Se}_3$  single crystal.

phases such as  $\text{MnBi}$ ,  $\text{MnSb}$  and  $\text{MnTe}$ ; none were observable. The Mn-doped  $\text{Bi}_2\text{Se}_3$  were a rhombohedral layered crystal structures;  $a = 4.106 \text{ \AA}$ ,  $c = 28.562 \text{ \AA}$ .

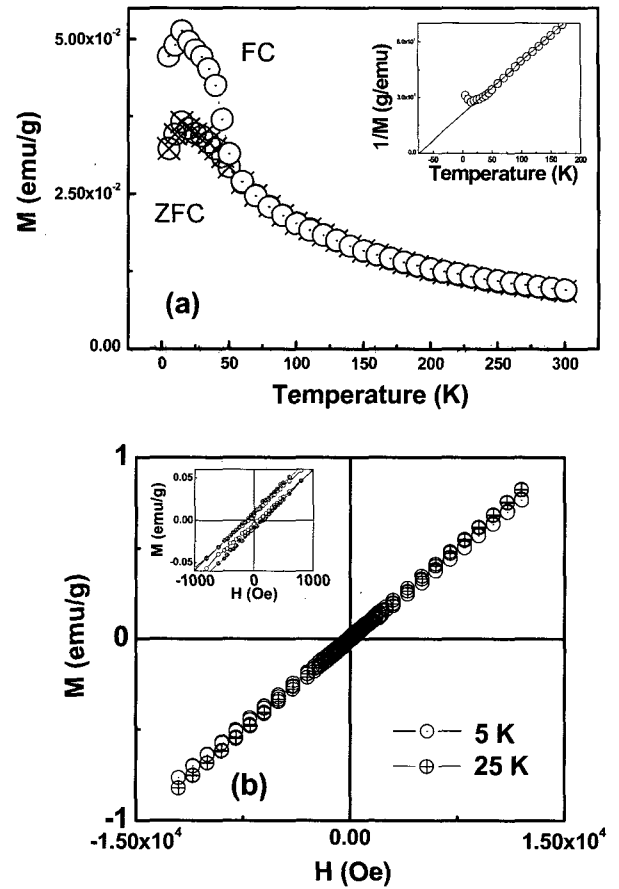
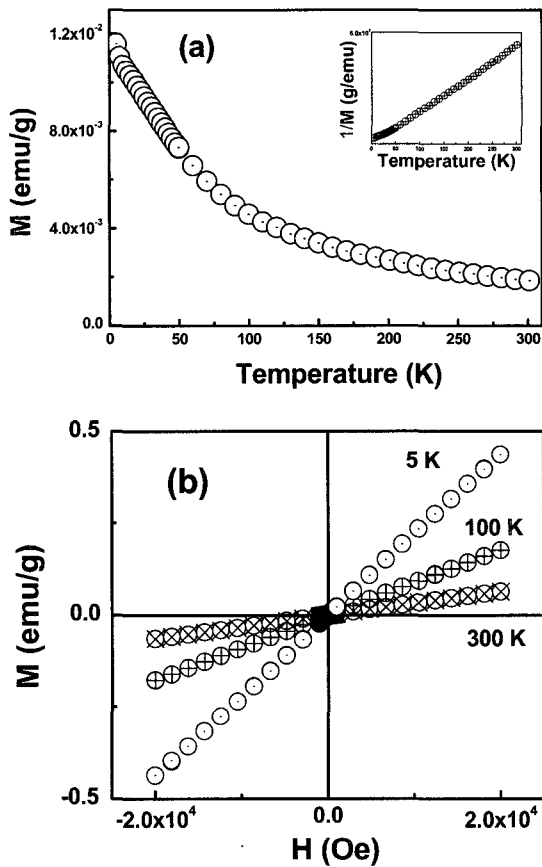


Fig. 3. (a) Temperature dependent magnetization ( $M$ ) and (b)  $M$ - $H$  (magnetic field) curves of  $\text{Bi}_{1.97}\text{Mn}_{0.03}\text{Se}_3$  single crystal. A reciprocal magnetization ( $1/M$ ) is shown in the inset of Fig. 3(a).

$\text{Sb}_{1.96}\text{Mn}_{0.04}\text{Se}_3$  was  $a = 11.565 \text{ \AA}$ ,  $b = 11.773 \text{ \AA}$ ,  $c = 3.971 \text{ \AA}$  with orthorhombic crystal structure. All of them were slightly smaller than those of  $\text{Bi}_2\text{Se}_3$  ( $a = 4.1396 \text{ \AA}$ ,  $c = 28.636 \text{ \AA}$ ), and  $\text{Sb}_2\text{Se}_3$  ( $a = 11.633 \text{ \AA}$ ,  $b = 11.780 \text{ \AA}$ ,  $c = 3.985 \text{ \AA}$ ) due to the smaller Mn atomic radius ( $1.40 \text{ \AA}$ ) than those of Bi ( $1.60 \text{ \AA}$ ) and Sb ( $1.45 \text{ \AA}$ ). The variations of lattice constants with Mn addition indicate the substitution of Mn in  $\text{Bi}_2\text{Se}_3$  and  $\text{Sb}_2\text{Se}_3$  lattices. We observed rod-like micro-sized structures in  $\text{Sb}_{1.96}\text{Mn}_{0.04}\text{Se}_3$  as shown in Fig. 2 [15].

We have investigated the magnetic properties of Mn-doped  $\text{Bi}_{1.97}\text{Mn}_{0.03}\text{Se}_3$  and  $\text{Sb}_{1.96}\text{Mn}_{0.04}\text{Se}_3$  single crystals using physical and magnetic property measurement systems (PPMS and MPMS, Quantum Design). Figure 3(a) shows the temperature dependent field-cooled and zero-field-cooled magnetization ( $M$ ) of  $\text{Bi}_{1.97}\text{Mn}_{0.03}\text{Se}_3$  single crystal in a 100 Oe magnetic field. The reciprocal temperature dependent  $M$  (the inset of Fig. 3(a)) and  $M$ - $H$  curve (Fig. 3(b)) indicate that  $\text{Bi}_{1.97}\text{Mn}_{0.03}\text{Se}_3$  shows spin glass. Figure 4 shows temperature dependent zero-field



**Fig. 4.** (a) Temperature dependent magnetization and (b) M-H curves of of  $\text{Sb}_{1.96}\text{Mn}_{0.04}\text{Se}_3$  single crystal. A reciprocal magnetization ( $1/M$ ) is shown in the inset of Fig. 4 (a).

cooled magnetizations (Fig. 4(a)) and M-H curves (Fig. 4(b)) of  $\text{Sb}_{1.96}\text{Mn}_{0.04}\text{Se}_3$  single crystal. It is observed that  $\text{Sb}_{1.96}\text{Mn}_{0.04}\text{Se}_3$  shows a typical paramagnetic behavior.

We now address the effects of some possible magnetic clusters such as MnTe, MnTe<sub>2</sub>, MnBi and MnSb on the observed magnetic properties. MnTe [16] and MnTe<sub>2</sub> [17] are antiferromagnetic materials with a Néel temperature of 320 and 86.55 K, respectively. The intermetallic MnBi [18] and MnSb [19] have FM ordering at 630 and 587 K, respectively. Thus, the observed spin glass property in Bi<sub>2</sub>Se<sub>3</sub> crystal may exclude effects from some possible clusters.

#### 4. Conclusion

We have grown Mn-doped Bi<sub>2</sub>Se<sub>3</sub> and Sb<sub>2</sub>Se<sub>3</sub> bulk

single crystals using vertical gradient solidification method. Both compounds had smaller lattice constants because of the smaller atomic radius of Mn than those of Bi (Sb). Mn-doped Bi<sub>2</sub>Se<sub>3</sub> and Sb<sub>2</sub>Se<sub>3</sub> have spin glass and paramagnetic properties, respectively.

#### References

- [1] David M. Rowe *et al.*, CRC Handbook of Thermoelectrics, CRC press, Section D-19 (1995).
- [2] Junwei Wang, Zhaoxiang Deng and Yadong Li, Mat. Res. Bul. **37**, 495 (2002).
- [3] D. Ferrand *et al.*, Phys. Rev. B **63**, 085201 (2001).
- [4] K. Ueda, H. Tabata, and T. Kawai, Appl. Phys. Lett. **79**, 988 (2001).
- [5] X. Liu, Y. Sasaki, and J. K. Furdyna, Appl. Phys. Lett. **79**, 2414 (2001).
- [6] H. Ohno, A. Shen, F. Matsukura, A. Oiwa, A. Endo, S. Katsumoto, and Y. Iye, Appl. Phys. Lett. **69**, 363 (1996).
- [7] M. E. Overberg, B. P. Gila, C. R. Abernathy, S. J. Pearton, N. A. Theodoropoulou, K. T. McCarthy, S. B. Arnason, and A. F. Hebard, Appl. Phys. Lett. **79**, 3128 (2001).
- [8] M. L. Reed, N. A. El-Masry, H. H. Stadelmaier, M. K. Ritums, M. J. Reed, C. A. Parker, J. C. Roberts, and S. M. Bedair, Appl. Phys. Lett. **79**, 3473 (2001).
- [9] D. Y. Park *et al.*, Science **295**, 651 (2002).
- [10] S. Cho, S. Choi, S. C. Hong, Y. Kim, J. B. Ketterson, B. J. Kim, and Y. C. Kim, Phys. Rev B **66**, 033303 (2002).
- [11] S. Cho *et al.*, Phys. Rev. Lett. **88**, 257203 (2002).
- [12] V. A. Kulbachinskii, A. Yu. Kaminskii, K. Kindo, Y. Marumi, K. Suga, P. Lostak, and P. Svanda, Physica B **311**, 292 (2002).
- [13] J. S. Dyck, P. Hájek, P. Lošťák, and C. Uher, Phys. Rev. B **65**, 115212 (2002).
- [14] J. Choi, S. Choi, J. Choi, Y. Park, H. M. Park, H. W. Lee, B. C. Woo, and Cho, Phys. Stat. Sol. (b) **241**(7), 1541-1544 (2004).
- [15] D. Wang, D. Yu, M. Mo, X. Liu, and Y. Qian, J. Crystal Growth **253**, 445 (2003).
- [16] C. Reig, V. Muñoz, C. Gómez, Ch. Ferrer, and A. Segura, J. of Crystal Growth **223**, 349 (2001).
- [17] J. M. Hastings, L. M. Corliss, and W. Kunmann, and D. Mukamel, Phys. Rev. B **33**, 6326 (1986).
- [18] J. B. Yang, W. B. Yelon, W. J. James, Q. Cai, S. Roy, and N. Ali, J. Appl. Phys. **91**, 7866 (2002).
- [19] P. Radhakrishna and J. W. Cable, Phys. Rev. B **54**, 11940 (1996).